

Design of Turkish Accelerator and Radiation Laboratory in Ankara (TARLA) facility injector magnets

Avni AKSOY*

Institute of Accelerator Technologies, Ankara University, Ankara, Turkey

Received: 04.01.2017

Accepted/Published Online: 08.02.2017

Final Version: 18.04.2017

Abstract: The installation of a high current thermionic gun-based injector capable to accelerate a maximum 1.5 mA electron beam at 250 keV and continuous wave (CW) for various bunch repetition rates has been continuing at the Turkish Accelerator and Radiation Laboratory in Ankara (TARLA) since 2014. The injector, which is based on totally normal conducting technology, will mainly consist of a thermionic DC electron gun, two stage bunch compressor cavities operating at 260 MHz and 1.3 GHz, one dipole magnet, five solenoid lenses and an additional one dipole magnet that is going to be used as spectrometer, and several steerer magnets. In this paper we discuss the design criteria of all magnets of the TARLA injector and present design results.

Key words: Accelerator magnets, solenoid magnet, dipole magnet

1. Introduction

The Turkish Accelerator and Radiation Laboratory in Ankara (TARLA), which has had continuous support from the Turkish Ministry of Development (TMD) since its conception in 2006, is designed as a multi-experiment facility providing a variety of accelerator-based radiation sources for users from various fields [1,2]. Based on a state-of-the-art superconductor technology, the current scope of the TARLA accelerator is designed to drive two free-electron laser (FEL) beamlines covering the range of 3–250 μm and one Bremsstrahlung line providing gamma radiation in the range of 1–30 MeV. With its high power electron beam, tunable FEL of high brightness in the mid- and far-infrared regime, and high intensity gamma radiation TARLA will be an outstanding research instrument for users from various fields like chemistry, physics, biology, material sciences, medicine, and nanotechnology.

The facility will mainly consist of an injector that provides a high current (up to 1.5 mA average current) CW electron beam at 250 keV, two superconducting (SC) accelerating modules separated by a bunch compressor in order to accelerate the beam to 40 MeV energy, and two independent optical resonator systems housing undulators with periods of $\lambda_{U90} = 90$ mm and $\lambda_{U25} = 25$ mm. The schematic view of the facility is given in Figure 1 and the main electron beam parameters of TARLA are given in Table 1 [3].

The main purpose of this study is to design suitable beamline magnets of the TARLA injector, which are going to be manufactured in Turkey and assembled at the Institute of Accelerator Technologies of Ankara University, where TARLA is currently under construction. During the design of the magnets, computer simulation technology (CST) software capable of applying 3D finite element methods (FEMs) as well as

*Correspondence: avniaksoy@ankara.edu.tr

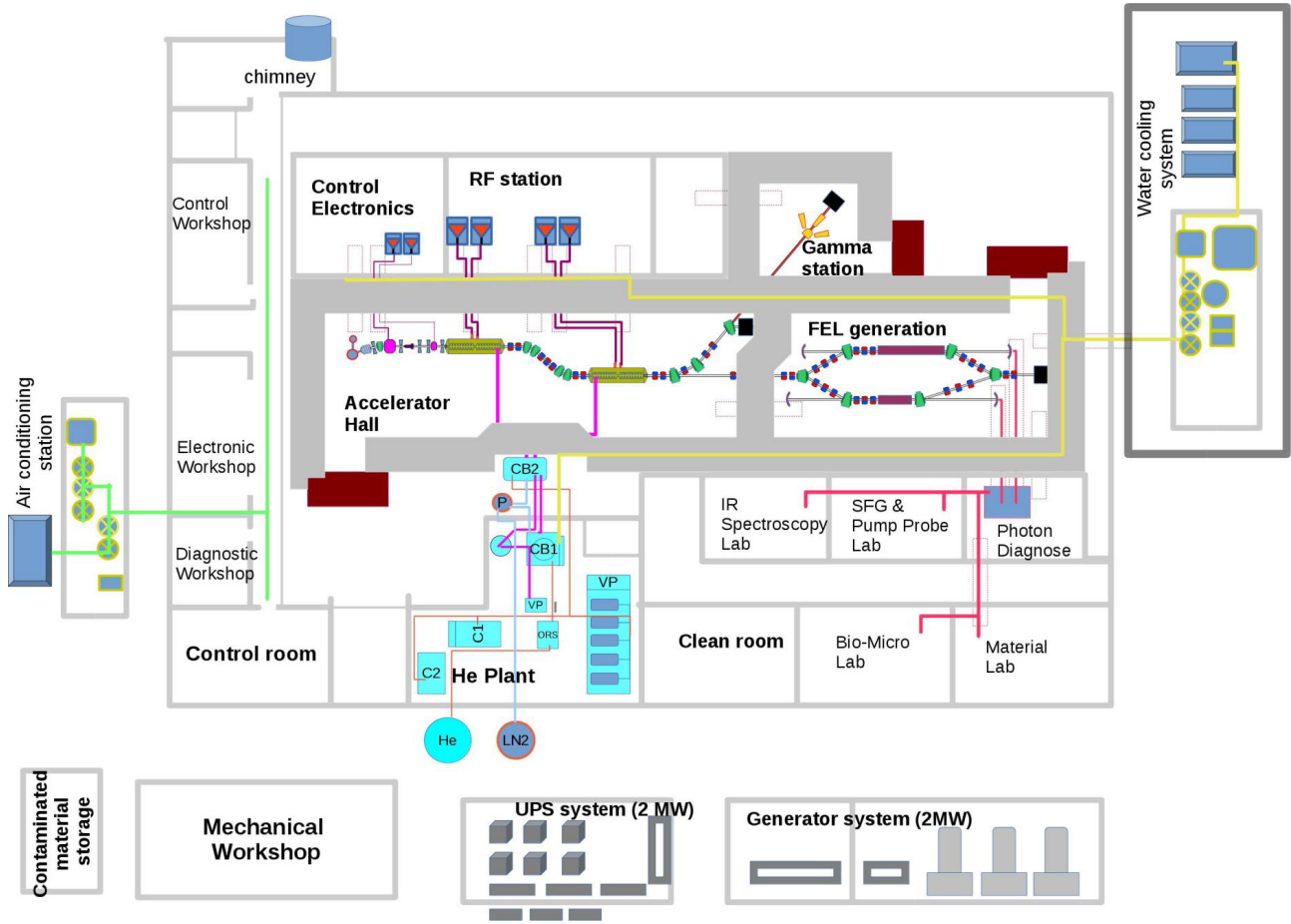


Figure 1. Schematic view of TARLA facility.

Table 1. Main electron beam parameters of TARLA.

Parameter	Unit	Value
Max. beam energy	MeV	40
Max. average beam current	mA	1.5
Horizontal emittance	mm mrad	< 15
Vertical emittance	mm mrad	< 12
Longitudinal emittance	keV ps	< 85
Bunch length	ps	0.4–6
Max. bunch repetition rate	MHz	104
Macro pulse duration	μ s	50 - CW
Macro pulse repetition rate Hz	Hz	1 - CW

analytical formulae was used [4]. In addition to magnet design, beam tracking was performed with ASTRA using the 3D field map created by CST [5].

1.1. TARLA injector

The TARLA injector, which is about 5.75 m long, will mainly consist of a thermionic triode DC electron gun providing a beam at 250 keV with requested bunch repetition, two normal conducting buncher cavities operating

at 260 MHz and 1.3 GHz, five solenoid lenses, one dipole magnet, and one spectrometer magnet (see Figure 2). The electron current is created at a tungsten dispenser cathode. The bunch structure of the beam is created with a modulated grid voltage located about $150 \mu\text{m}$ from the cathode. For a nominal micropulse repetition rate (13 MHz) the bunches have about 600 ps full-width half-maximum (FWHM) length. They are compressed via velocity bunching in the drift following the energy modulation by the subharmonic buncher (SHB) and fundamental buncher (FB). The FB introduces enough energy modulation in order to generate longitudinal waist inside the first cell of the first SC cavity [3].

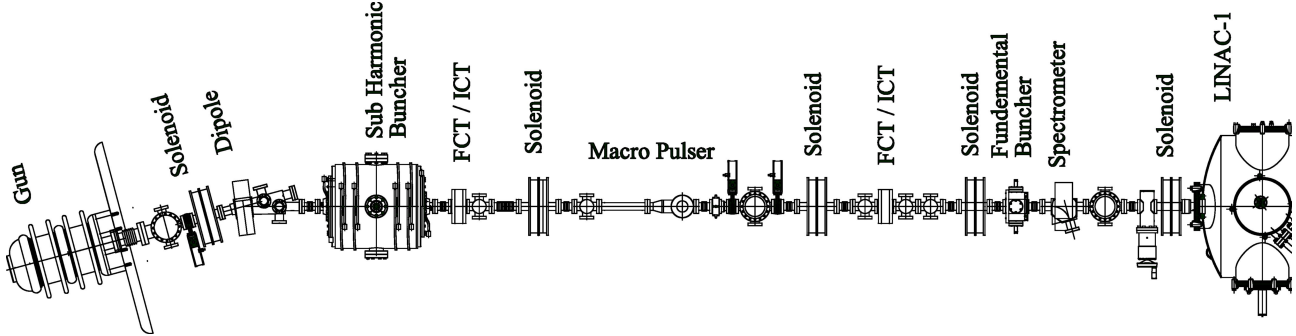


Figure 2. Layout of TARLA injector.

One of the major problems with transporting low energy bunches is the emittance growth and energy spread driven by space charge. Therefore, the injector section should be kept short to minimize the emittance growth due to space charge effects. In addition, this reduces the phase jitter due to fluctuations of the gun high voltage. On the other hand, a short injector requires a large energy modulation for the bunching, which may increase chromatic effects of the focusing solenoids. One has to find a suitable compromise that minimizes the emittance growth in all longitudinal and transverse directions.

With beam dynamics simulation it was found that five solenoid magnets would be sufficient for transporting the beam through the injector [2,3]. The axis of the beamline just after gun has a bend about 15° in order to avoid the field emission current from the SC cavities to back-bombard the cathode. A spectrometer has been foreseen just after the FB in order to diagnose longitudinal phase space during operation of the machine.

2. Magnet design

The optical elements of the beam transport lines can be classified as magnetic and electric devices. In the case of high-energy beams ($v \approx c$), magnetic elements are preferred. For example, the force created with magnetic field of 1 T is equivalent to the force from an electric field of 300 MV/m; however, the magnetic field of 1 T can easily be produced while the electric field of 300 MV/m is almost impossible to produce with an electrostatic device. In low-energy beam transport systems, where the beam velocity is low, the achievable forces are comparable; however, other factors, such as size, cost, power consumption, and the effects of beam space-charge compensation, come into play. The common magnetic beamline elements that are used to build beam transport systems are solenoid, dipole, and quadrupole magnets and electrostatic devices are immersion and einzel lenses [6]. Taking into account the size, cost, and power consumption factors mentioned above, magnetic focusing elements have been chosen for the TARLA injector. For deflecting the beam dipole magnets are used while for the focusing only solenoid magnets are used because the quadrupole magnets are generally preferred for high energy beams.

In general, in order to concentrate the field into required region, soft iron yoke of high permeability is used. This method guarantees high field quality on the requested region and also reduces electric power consumption. On the other hand, if the required field strength either is very small ($B \ll 0.1$ T) or above saturation level of iron ($B > 2$ T) air coil magnets are used [7]. In addition, if one requires uniformity of field (i.e. uniform magnetic field between poles of a dipole and low high order term components) iron yoke has to be used to ensure field quality.

2.1. Solenoid magnet

A solenoid magnet consists of rotationally symmetric coils surrounding the beam tube. It is used to create a longitudinal magnetic field that has a peak at the center of the beam tube. The magnetic field is pure longitudinal in the inner part of the coil and it contains radial components in the outer part of the coil. As it can easily be seen from Lorentz force the particles that are moving on the axis do not feel any force. The particles moving off-axis experience azimuthal force due to the radial component of the field during entrance and exit of the solenoid and change azimuthal location. Thus the particles that have azimuthal velocity will feel radial force due to longitudinal field inside the coil. The focal length of the coil is given by

$$\frac{1}{f} = \int \left(\frac{eB_s}{2p} \right)^2 ds \quad (1)$$

where e is the electron charge, B_s is the longitudinal magnetic field, p is the particle momentum [6]. As it can be seen from Eq. (1) the solenoids have small focal length when the particle momentum is small. For the electron that has momentum $p > 1$ MeV/c quadrupoles are more effective lenses for focusing the beam.

As shown in Figure 2, five solenoid magnets will be used for focusing the beam through the TARLA injector. We propose solenoids to be identical and to have two opposite polarity coils so that they will not cause the beam to rotate, thus minimizing emittance growth. Figure 3 shows the mechanical design and field map on cross section of the solenoid for maximum current.

The calculation of the designed solenoid was performed using CST software. We used $1155 \text{ A} \times \text{turns}$ ($11 \times 30 \times 3.5 \text{ A}$) and simulation shows that it has maximum 400 G magnetic field, which corresponds about 25 cm focal length at 250 keV beam energy. Figure 4 shows the simulations results of TARLA solenoids. As it can be seen on the left-hand side figure the effective length of the solenoid is about 7 cm and the maximum field on the axis is about 400 G. On the right-hand side of the figure it is seen that even if 7 A current is applied to the coils the iron is still below saturation level of 2 T.

Another crucial subject in the design of magnets is the cooling requirement of the coil. Since the copper wire will have a resistance of $R = \rho l/A$, where ρ is the resistivity of wire (for copper at room temperature $\rho \approx 1.8 \times 10^{-8} \text{ m}$), l is the length of the cable, and A is the area of cross-section of cable. Thus the coil constructed with copper wire will act as a heater inside the solenoid. The heat shall be removed from the coil so that the temperature of the wire will remain constant. Generally if the current density is $j = 2 \text{ A/mm}^2$ water cooling is used via passing water inside the wire of duct shape. In our case although we have about $j = 0.5 \text{ A/mm}^2$ current density we need to check the temperature rise because the coil is covered with soft iron that can prevent heat transfer from coil to air. Figure 5 below shows the saturated temperature rise inside the solenoid coil and heat transfer from the solenoid to the air. It can be seen in the figure that the iron cover allows heat transfer and the temperature is stable at 62 degrees for maximum current, which is acceptable for long run operation.

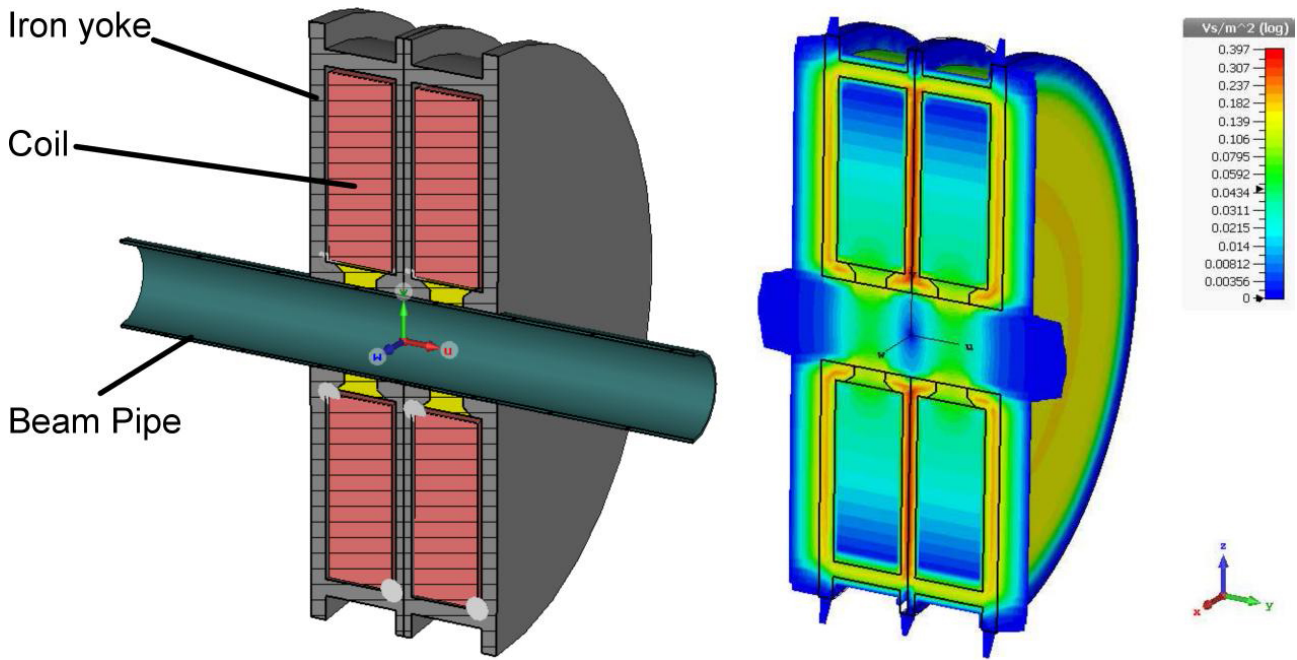


Figure 3. Mechanical model of solenoid and field map on planar surface.

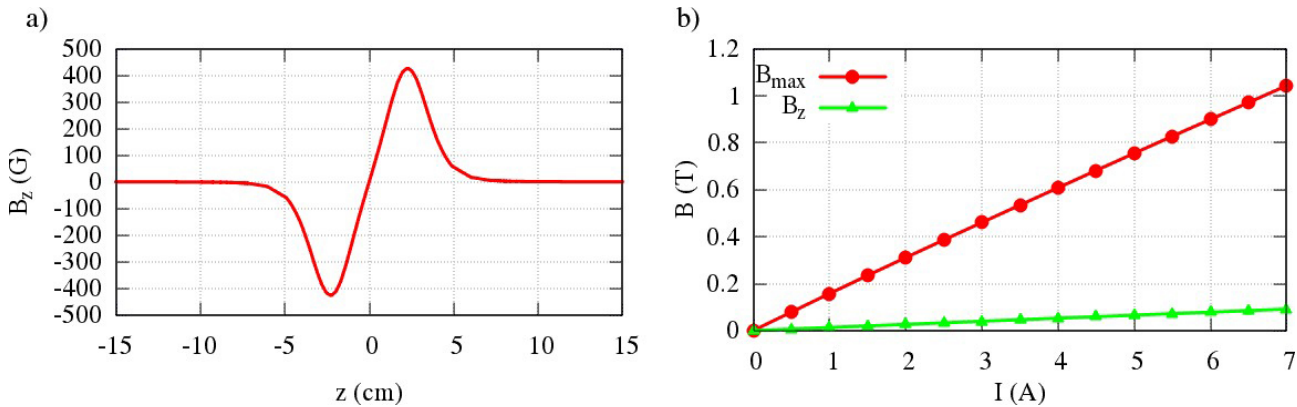


Figure 4. a) Longitudinal magnetic field at the axis of solenoid for nominal current, b) magnetic field inside and axis of the solenoid versus the coil current.

2.2. Dipole and spectrometer magnet

As discussed earlier, to avoid the field emission being stored on the cathode the axis of the TARLA gun was rotated 15° with a bending magnet located just after the gun (see Figure 2). Additionally, to diagnose the longitudinal parameters of the beam during operation an additional bending magnet after the FB is going to be used as spectrometer.

Dipole magnets are the most commonly used elements for bending the beam direction or deflecting the beam or steering the beam on transport lines. Dipole magnets are used to create a uniform field between two poles that is excited by a current flux in the coils. In other words, according to the right-hand rule the magnetic dipole is created by coil windings and the direction of the magnetic field is adjusted to the transverse direction

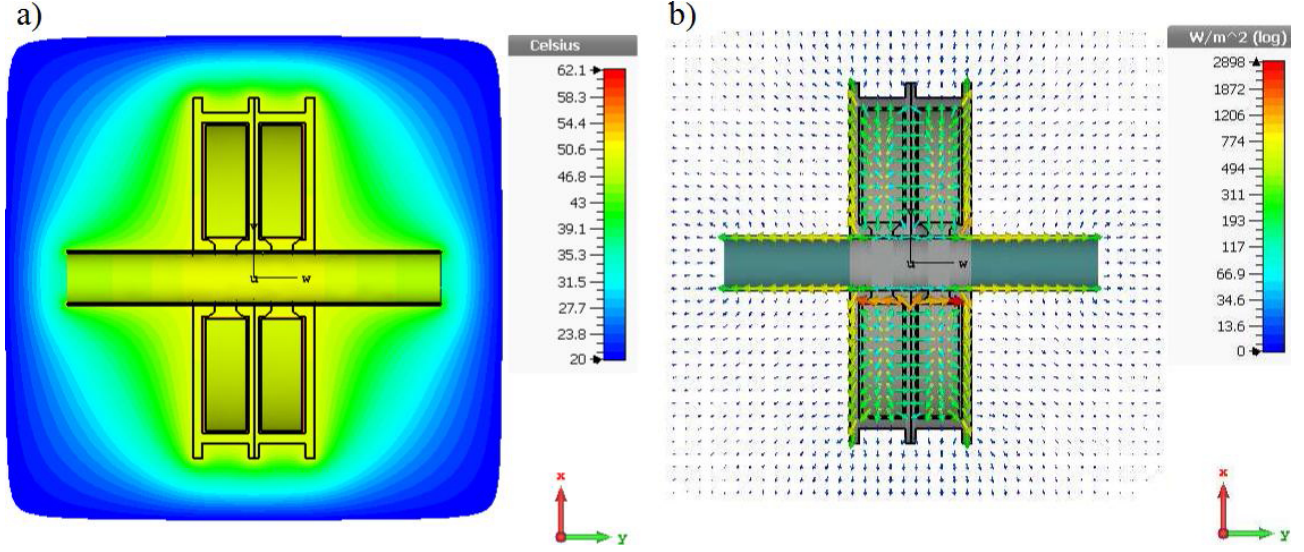


Figure 5. a) Saturated temperature of solenoid magnet, b) heat transfer through the environment from solenoid.

of the beam's moving path. A beam in a magnetic field follows a circular trajectory with bending radius

$$\frac{1}{\rho} [m^{-1}] = e \frac{B}{p} = 299.8 \frac{B_d [T]}{p [\frac{MeV}{c}]} \quad (2)$$

where B_d is the magnetic field between poles and p is the particle momentum [7]. The magnetic field of a dipole can be approximated as

$$B_d = \frac{\mu_0 n I}{h} \quad (3)$$

where μ_0 is the permeability of air, n is the number of turns of the coil, I is current, and h is the distance between poles (gap height) [8]. One should note that the formula is only approximate; it ignores the geometry, saturation of iron, and fringe fields. However, it gives an assumption between the range of current and the height of gap.

As it can be seen in Eq. (2), the bending radius and therefore the bending angle depend on the particle momentum, which will never be identical for the particles within a bunch. In other words, the bending angle momentum correlation in a bending magnet lets those magnets be used as a spectrometer. In the beam physics literature momentum dependence of particle motion is called dispersion and if the energies of particles within a bunch are different from the reference energy each dipole magnet introduces dispersion [7]. Since the energy spread just after the gun is very low the dispersion can be ignored in the background of a rather large geometrical emittance. On the other hand, the buncher cavities that are used for compressing bunches longitudinally via ballistic bunching introduce large energy spread within the bunch; thus the dipole magnet located after the FB can be used as spectrometer and the dispersion cannot be neglected on this position.

Taking into account these considerations, in order to keep roundness of beam after the gun a dipole magnet with equal focusing effect in both horizontal and vertical directions has been designed by optimizing the fringing fields. By using Eq. (2) it can easily be computed that the required magnetic field at a dipole magnet with 12 cm length and bending angle of 15° is about 40 G for an electron beam that has kinetic energy of 250 keV. According to Eq. (3), required total current can be found about $150 \text{ A} \times \text{turns}$ for a dipole that

has 42 mm gap height. Since the magnetic field of the first dipole is less than 100 G, having a sharp edge field is rather difficult, and a Clamped Rogowski type pole design has been used in order to optimize fringe fields [8]. To have easy access to the beam pipe C-type of bending magnet was chosen. Figure 6 shows the mechanical model and 3D magnetic field distribution.

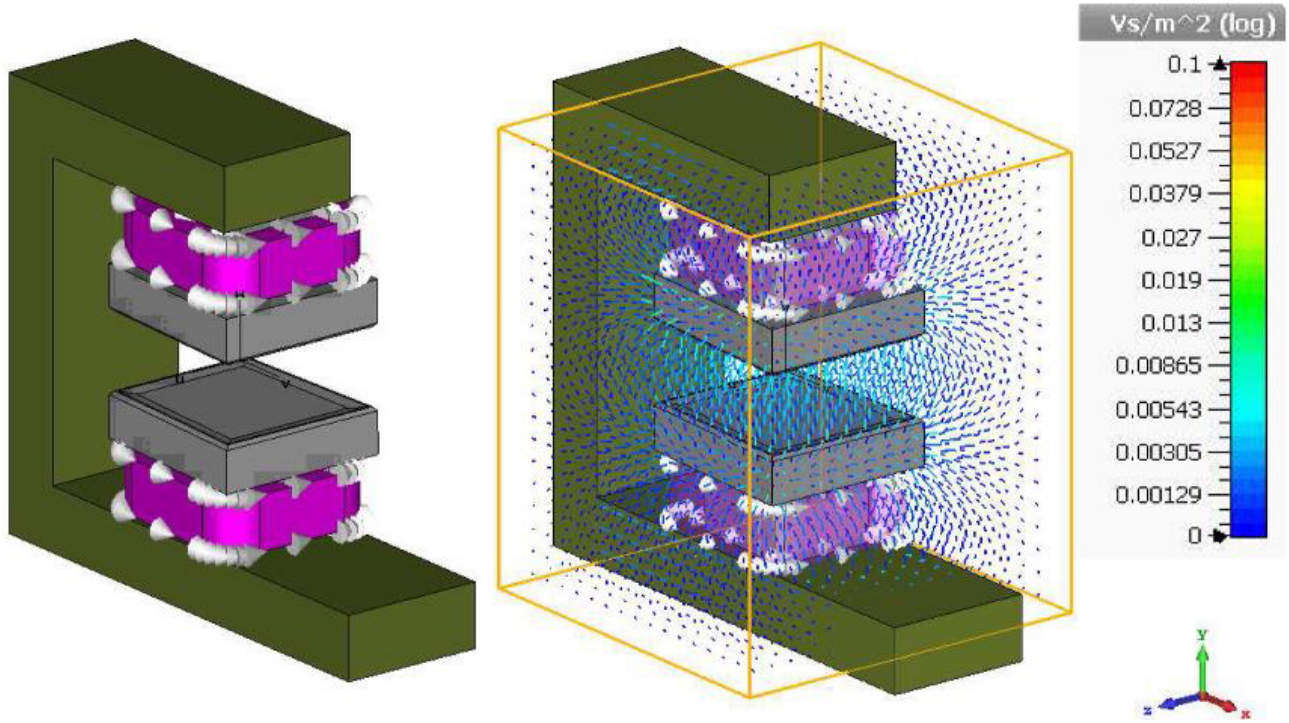


Figure 6. Mechanical model of dipole magnet and its 3D magnetic field lines.

We used double coil with $75 \text{ A} \times \text{turns}$ ($n_{hor} \times n_{ver} \times I_{wire} = 5 \times 10 \times 1.5 \text{ A}$) to create a 40 G magnetic field between the poles of the dipole. Figure 7 shows the dipole field along beam path (a) and field distribution between poles. As it can be seen the field strength drops to almost zero at about 10 cm far from the poles.

The field homogeneity is another important parameter of a magnet, especially for the dipoles on low-energy beam transport systems. It is described as the variation of magnetic field on the interested region distance such as $|(B(y=0, z, x) - B_0)/B_0|$, where B_0 is the field at the origin of the magnet. The homogeneity is generally determined according to the energy spread, transverse size, and correlated energy spread of the beam to be transported. The field homogeneity between poles of the dipole is about 1%, which is acceptable for these field strengths and fulfills the requirement of the TARLA injector transport system.

We also checked beam transport through the dipole magnet using Astra code with a 3D field map created by CST. Figure 8 shows the transverse beam distribution before and after the dipole magnet and beam phase space before and after the dipole magnet. As it can be seen the beam is still round after the dipole magnet and the horizontal emittance is not changed much due to dispersive effects.

Similar considerations like dipole magnet were taken into account during the design of the spectrometer magnet. In order to bend the beam 75° on a dipole magnet that has bending radius of 115 mm one can easily compute that the required dipole field is about 160 G. To create 160 G magnetic field strength on a dipole with gap spacing of 42 mm one can compute the required total current as about $550 \text{ A} \times \text{turns}$ using Eq. (3).

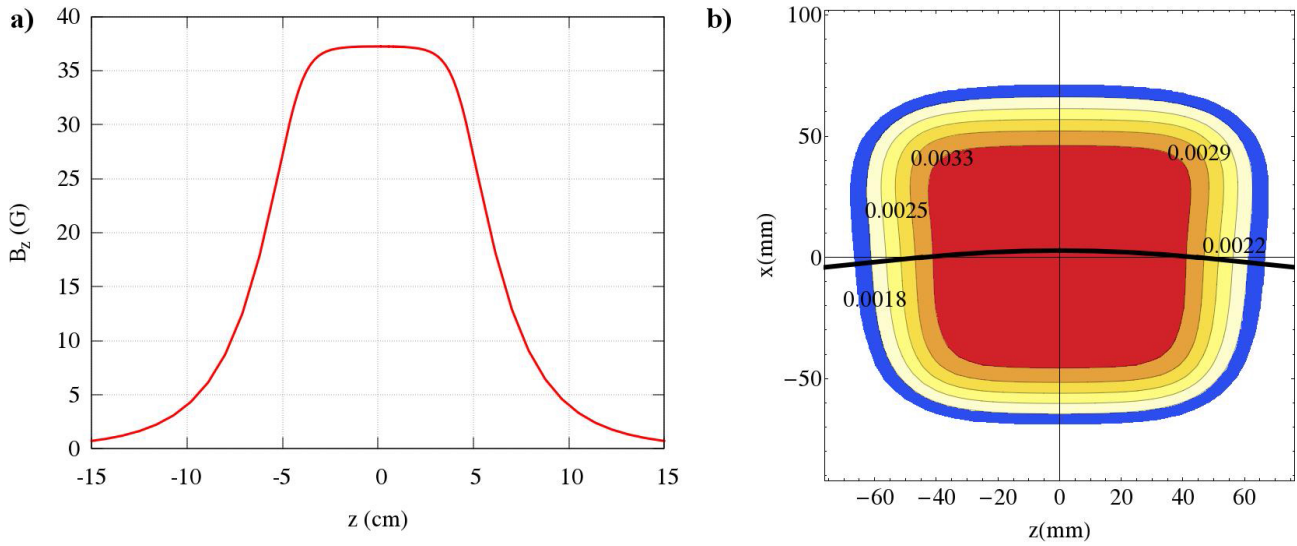


Figure 7. a) Vertical magnetic field along beam path, b) vertical magnetic field distribution between dipole poles, black line represents beam path between poles.

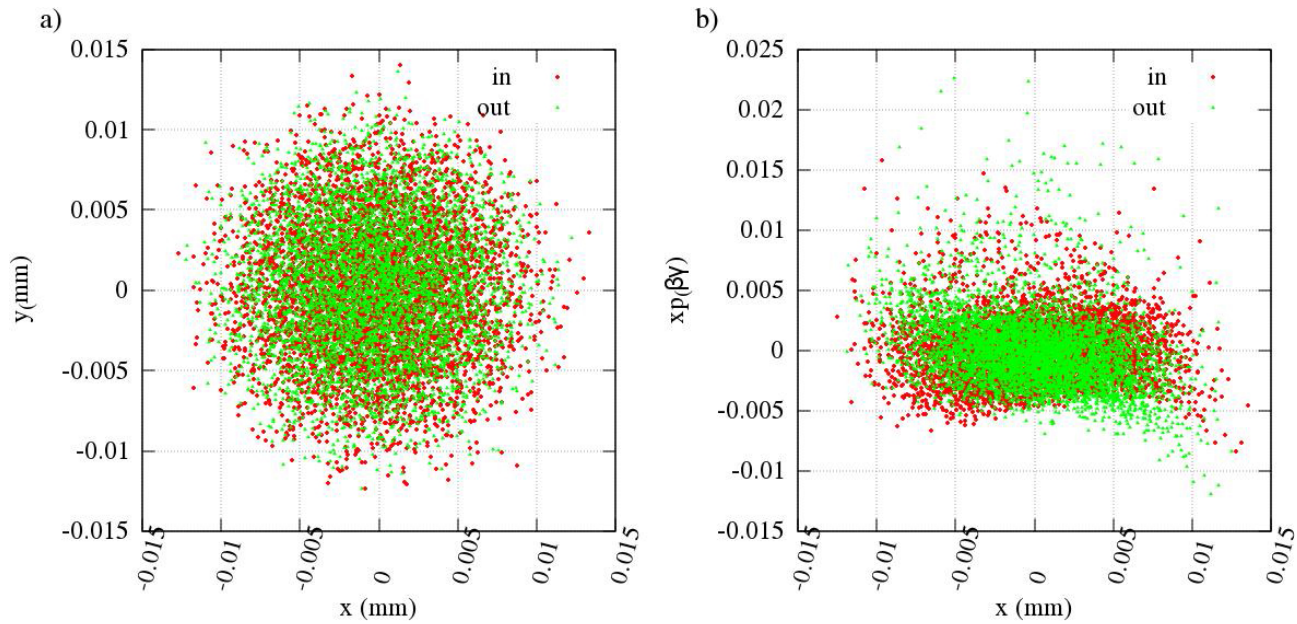


Figure 8. a) Transverse beam distribution before and after dipole, b) horizontal phase space before and after dipole. Red colors represent macro particles before dipole, green colors represent macro particles after dipole magnet.

Since the beam quality after the spectrometer is as not strict as the first dipole magnet we did not make any optimization for fringe files in order obtain a specific beam transport assessment. Figure 9 shows the mechanical model and 3D magnetic field distribution of the spectrometer magnet. As it can be seen, similar to the dipole magnet, to have easy access to beam pipe C type of magnet was designed.

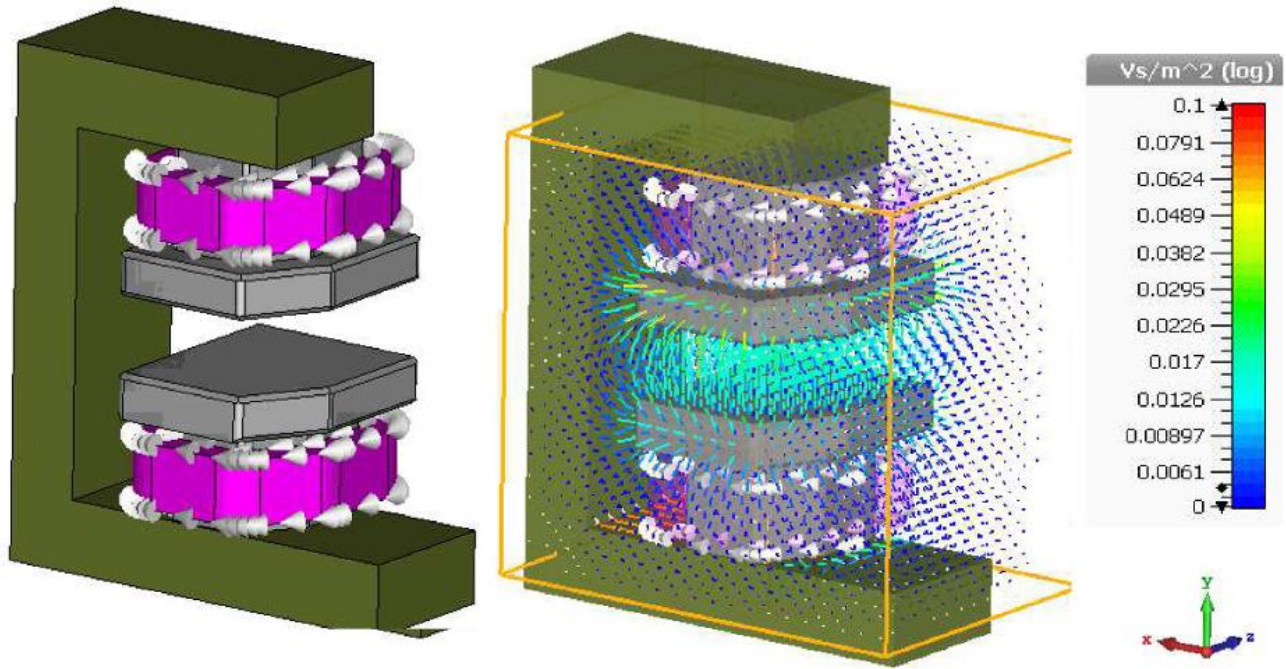


Figure 9. Mechanical model of spectrometer magnet and its 3D magnetic field lines.

A double coil with $288 \text{ A} \times \text{turns}$ ($n_{hor} \times n_{ver} \times I_{wire} = 6 \times 12 \times 4 \text{ A}$) was used to create a 160 G magnetic field between the poles of the spectrometer. Figure 10 shows the vertical magnetic field along beam path (a) and field distribution between poles (b). As it can be seen the field strength drops to almost zero at about 15 cm from the dipole poles (sharp edge) and the field homogeneity between poles is about 1%.

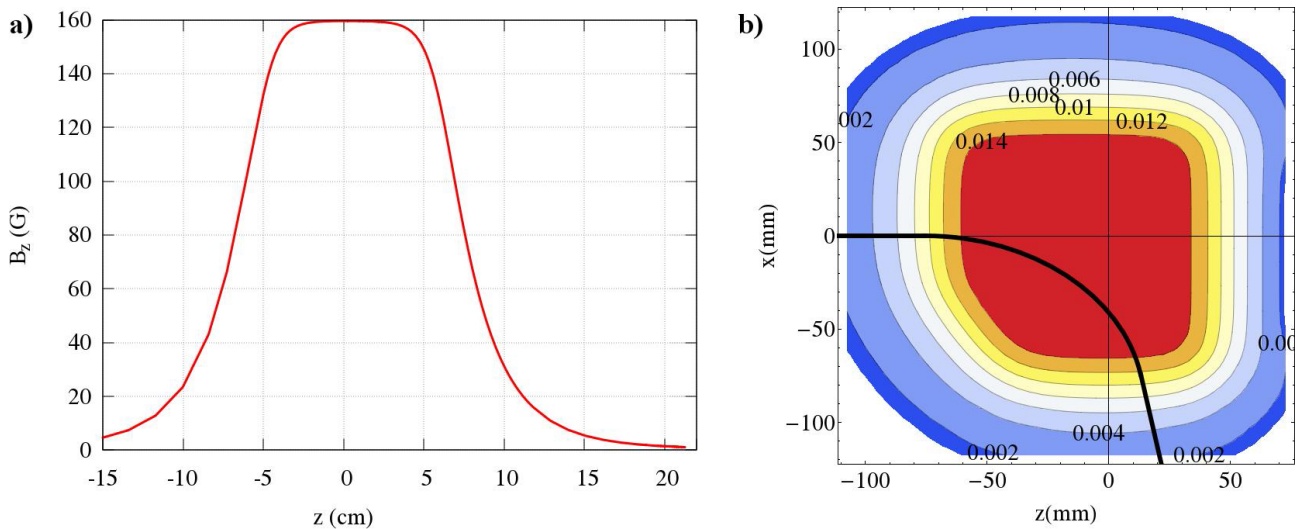


Figure 10. a) Vertical magnetic field along beam path, b) vertical magnetic field distribution between the poles (black line represents beam path).

As discussed earlier, if the current density j is above 2 A/mm^2 water cooling is required on the wire of the coil. For both dipole and spectrometer magnets the current density is still far below this limitation (i.e. the

current density for spectrometer is $j = 0.5 A/mm^2$). The coils are not surrounded by any other material; thus we regard heat simulation as unnecessary for dipole and spectrometer magnets.

3. Conclusion

Particle accelerators are known key drivers for R&D, innovation, and socio-economic development and magnet technology is one of the key technologies for building blocks of construction of accelerator systems. The demand for high fields at large bore magnets, solenoid, dipole, quadrupole and sextupole configurations, and field quality are example challenges that are being met by engineers and scientists developing magnets. The main objective of this study is the design of TARLA magnets and their manufacture in Turkey for enabling the involvement of Turkish industry in the international accelerator market as well as creating a base future relevant project of Turkey such as TURKAY [9] after TARLA.

In this paper we have described the design results of solenoid, dipole, and spectrometer magnets that are going to be used in the TARLA injector in accordance with requirements for FEL operation. By using simple analytical formulae draft parameterization has been performed to derive a list of main magnet parameters. Using 3D FEM we optimized magnets in term of field homogeneity, fringe fields, and heat load. Finally particle tracking has been performed using the field map created by 3D tool. The main parameters of the designed magnets are summarized in Table 2.

Table 2. Design parameters of TARLA injector magnets.

Parameter	Parameter	Solenoid	Dipole	Spectrometer
Maximum field	G	400	100	200
Bending radius	mm	NA	450	90
Bending angle	Degree	NA	15	75
Entrance/exit angle	Degree	NA	2.5/2.5	0/15
Focusing length	mm	250	NA	NA
Pole gap/pipe radius	mm	42	42	42
Effective length	mm	70	100	150
Pole profile - entrance/exit	#	NA	Rogowski	Sharp edge
Pole profile - sides	#	NA	Sharp edge	Sharp edge
Homogeneity within ± 30 mm	%	NA	1%	1%
Pole material	#	A1006	A1006	A1006
Yoke material	#	ST37	ST37	ST37
Coil type	#	Circular	Circular	Circular
Conducting material	#	Cu	Cu	Cu
Conductor dimensions	mm	3	3	3
Cooling type	#	Air cooled	Air cooled	Air cooled
Number of turns per coil	#	330	15	72
Max. required current	A	3.5	1.5	4
Voltage	V	20	20	20

The original design of the electron gun, buncher cavities, and superconducting accelerators of TARLA are based on the designs for the Radiation Source ELBE [10]. They are slightly improved by the TARLA team for higher bunch charge, higher repetition rate, and more stable beam operation. On the other hand, the beam transport system of TARLA is totally different from the ELBE project and therefore there are no similarities between magnets of two facilities.

The TARLA facility is currently under construction at the Institute of Accelerator Technologies of Ankara University. The thermionic triode DC electron gun has been operating since 2014. The cryoplant of the facility is installed and it is under commission currently. Two superconducting accelerating modules will be delivered by beginning of 2017. The 20 MeV section of the accelerator is planned to be operated in 2017 and the second part will be operated in 2018. The first lasing is planned to be achieved in 2019 and provided to users in the same year. A laser experimental station with conventional laser sources is planned to be operational by 2017.

Acknowledgment

This work was supported by the Turkish Republic Ministry of Development with grant no. DPT2006K120470.

References

- [1] Aksoy, A.; Karsh, Ö.; Yavaş, Ö. *Infrared Phys. Techn.* **2008**, *51*, 378-381.
- [2] Aksoy, A.; Karsh, Ö. *TARLA Design Report*; Ankara University, Institute of Accelerator Technologies, Ankara, Turkey, 2015.
- [3] Aksoy, A.; Lehnert, U. *Nucl. Instr. Meth. Phys. Res. A* **2014**, *762*, 54-63.
- [4] Computer Simulation Technology, <https://www.cst.com/>.
- [5] Floettmann, K. *ASTRA User Manual*; DESY, Hamburg, Germany, 2011.
- [6] Liebl, H. *Applied Charged Particle Optics*; Springer: Berlin, Germany, 2008.
- [7] Wiedemann, H. *Particle Accelerator Physics*; Springer: Berlin, Germany, 2007.
- [8] Brandt, D. In *CAS-CERN Accelerator School Proceedings: Specialized Course on Magnets*, Bruges, Belgium, 16–25 June 2009.
- [9] Nergiz, Z. *Nucl. Instr. Meth. Phys. Res. A* **2015**, *795*, 140-143.
- [10] Gabriel, F.; Gippner, P.; Grosse, E.; Janssen, D.; Michel, P.; Prade, H.; Schamlott, A.; Seidel, W.; Wolf, A.; Wunsch, R. *Nucl. Instr. Meth. Phys. Res. B* **2000**, *161-163*, 1143-1147.